Dissolution and Characterization of Regenerated *Antheraea pernyi* Silk Fibroin

HAEYONG KWEON, YOUNG HWAN PARK

Department of Natural Fiber Science, Seoul National University, Suwon 441-744, South Korea

Received 4 April 2000; accepted 5 December 2000

ABSTRACT: Dissolution of *Antheraea pernyi* silk fiber was carried out in a calcium nitrate solution with various dissolving conditions. The solubility was significantly dependent on the concentration of calcium nitrate, dissolving temperature, and time. The proper conditions of dissolution were found as 7*M* calcium nitrate, 100°C temperature, and 3 h dissolving time. The aqueous solution of *A. pernyi* silk fibroin was composed of a mixture of polypeptides with several molecular weights above 14 kDa. FTIR and XRD showed that regenerated *A. pernyi* silk fibroin was composed of an α-helix as well as a random-coil conformation while silk fiber had a traditional β-sheet structure. The endo–exo transition in the temperature ranges of 228–232°C also supports these conformations of regenerated silk fibroin film. TGA and DTG curves showed that the thermal decomposition of regenerated *A. pernyi* silk fibroin proceeded by three steps, not dependent on the conformation. The mechanical damping peaks (tan δ) appeared about 227°C with a minor shoulder maximum about 240°C, which were somewhat lower than those of tussah silk fiber. © 2001 John Wiley & Sons, Inc. J Appl Polym Sci 82: 750–758, 2001

Key words: *Antheraea pernyi* silk fibroin; dissolution; calcium nitrate; conformation; thermal behavior; mechanical damping

INTRODUCTION

A silk protein polymer, produced by silkworms, is classified into two general groups: domestic (*Bombyx mori*) and wild type (*Antheraea pernyi*, etc.). The former has been widely studied as a source of biomaterials to be used in biotechnological and biomedical fields because it has good blood compatibility, oxygen permeability, and so on.[1,2] Dissolution of silk fibroin was often required when nontextile applications were concerned, such as in the form of a porous membrane, powder, and gel.

Fibroin within the posterior division of the silk gland in full-grown larvae of the silkworm is an aqueous solution. Once the silk fiber was solidified though a spinning process from the silkworm, it became a well-oriented and highly crystallized polymer. Silk fiber behaves like a thermoset polymer, although it is not all crosslinked. Therefore, concentrated chaotropic salts, which destabilize proteins in solution and increase the solubility of proteins,[3] are required to dissolve *B. mori* silk fiber, such as calcium chloride and lithium bromide. The prior solvents that have been used to dissolve *B. mori* silk fibroin had difficulty dissolving *A. pernyi* silk fibroin due to its strong resistance of chemicals. The main conformation of *A. pernyi* silk fiber is an extended antiparallel β-sheet structure of a hydrogen bond among the chains through —C═O and —NH groups. This intermolecular bonding is sufficiently strong to prevent the separation of the molecules and,

Correspondence to: H. Kweon.

Journal of Applied Polymer Science, Vol. 82, 750–758 (2001)

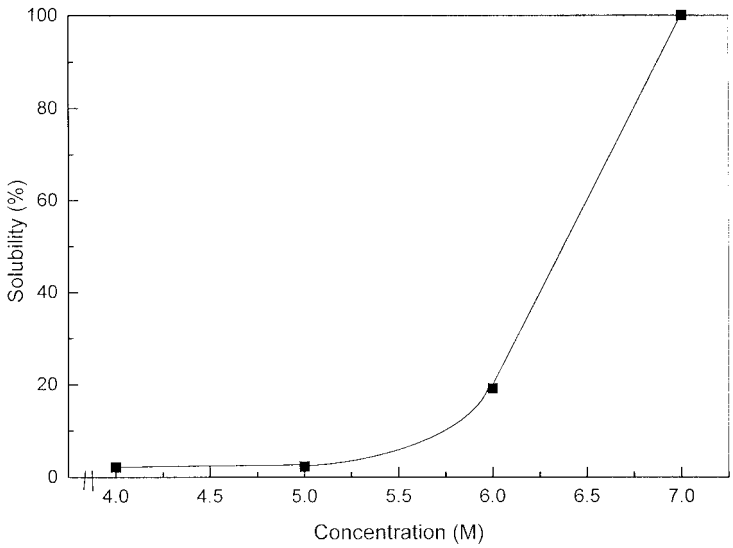

Figure 1 Effect of concentration of calcium nitrate on the solubility of *A. pernyi* silk fiber treated at 110°C for 3 h.

hence, to resist their dissolution into various chemicals.

The dissolution of *A. pernyi* silk fibroin as well as the properties of regenerated fibroin are important from the practical viewpoint of silk fibroin application for nontextile materials such as for wound dressing, artificial skin, matrix for cell culture, and drug delivery. Previously, we screened chaotropic salts such as magnesium, zinc, and calcium nitrate to obtain regenerated silk fibroin film.[4] The concentrations of regenerated silk fibroin in solutions that have been dialyzed to remove most of the salts have been limited because of the low solubility of silk in pure water.[5] The removal of ions may result in the aggregation of the silk molecules from their soluble state. According to our preparatory experiments, most regenerated silk solutions except calcium nitrate became unstable during dialysis. The object of the present work was to prepare regenerated *A. pernyi* silk fibroin from a calcium nitrate solution and to investigate the structural

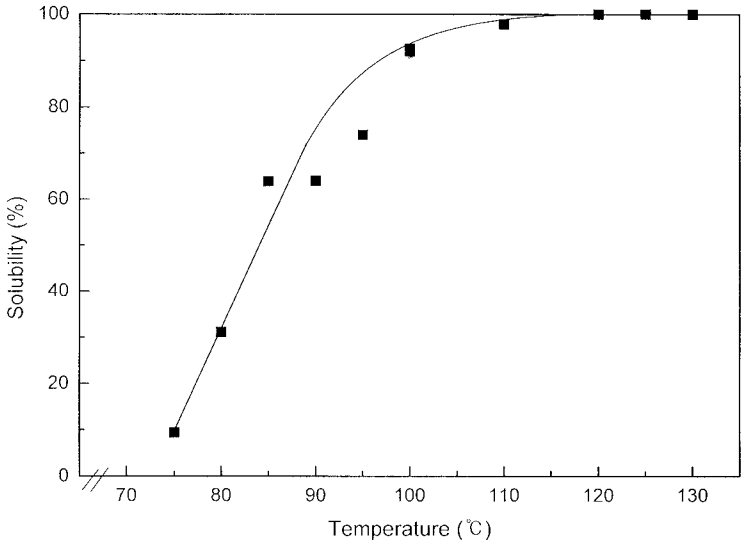

Figure 2 Effect of temperature on the solubility of *A. pernyi* silk fiber treated with 7*M* calcium nitrate for 3 h.

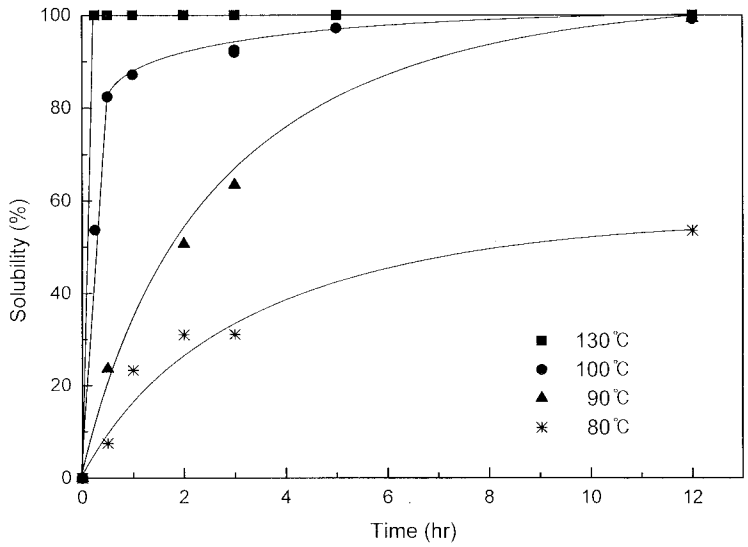

Figure 3 Effect of time on the solubility of *A. pernyi* silk fiber treated with 7*M* calcium nitrate.

and thermal properties of regenerated fibroin film using Fourier transform infrared (FTIR), X-ray diffraction; (XRD), differential scanning calorimetry (DSC), thermogravimetric analysis (TGA), and dynamic mechanical thermal analysis (DMTA).

EXPERIMENTAL

Materials

A. pernyi silk fibers were degummed using an enzymatic degumming method, followed by dissolving them in a calcium nitrate solution. *A. pernyi* silk fibers were first treated with the degummed solution (Alcalase 2.5L form Novo Industries Co., 1 g/L; sodium bicarbonate, 5 g/L; and nonionic surfactant (Ansan, Korea), 1 g/L) at 55°C for 60 min. The degummed fibers were washed in the mixture solution of the nonionic surfactant, 2 g/L, and sodium hydrosulfite, 5%, on the weight of the fiber and then thoroughly rinsed in warm distilled water. They were dried at room temperature and stored in a desiccator prior to use.

Solubility

To determine the optimum conditions for the dissolution of *A. pernyi* silk fiber, several dissolution parameters, such as the concentration of salt, treatment temperature, and treatment time under stirring, were studied. The weight of the undissolved silk fibroin was filtered through nonwoven fabrics and weighed. The solubility was calculated with the following equation:

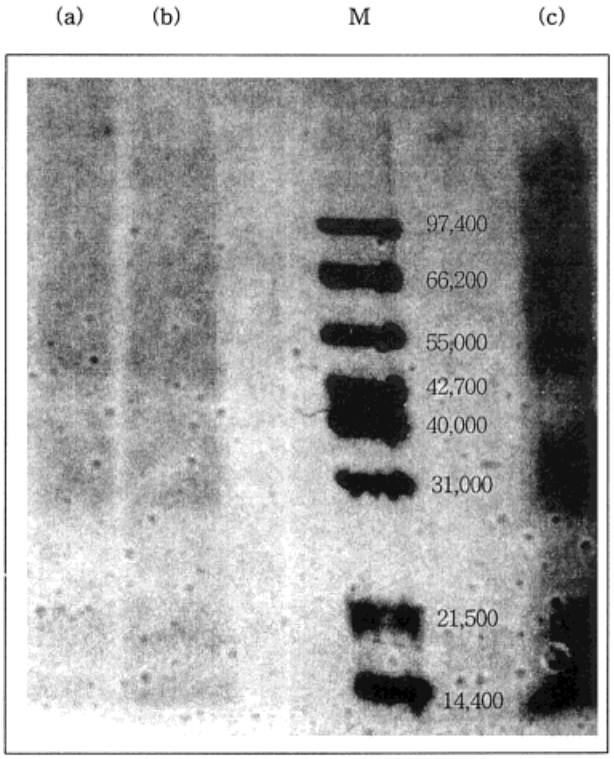

Figure 4 SDS–PAGE patterns of regenerated *A. pernyi* silk fibroin dissolved in 7*M* calcium nitrate at 100°C for 3 h; *M*: molecular weight marker; (a–c) regenerated solution.

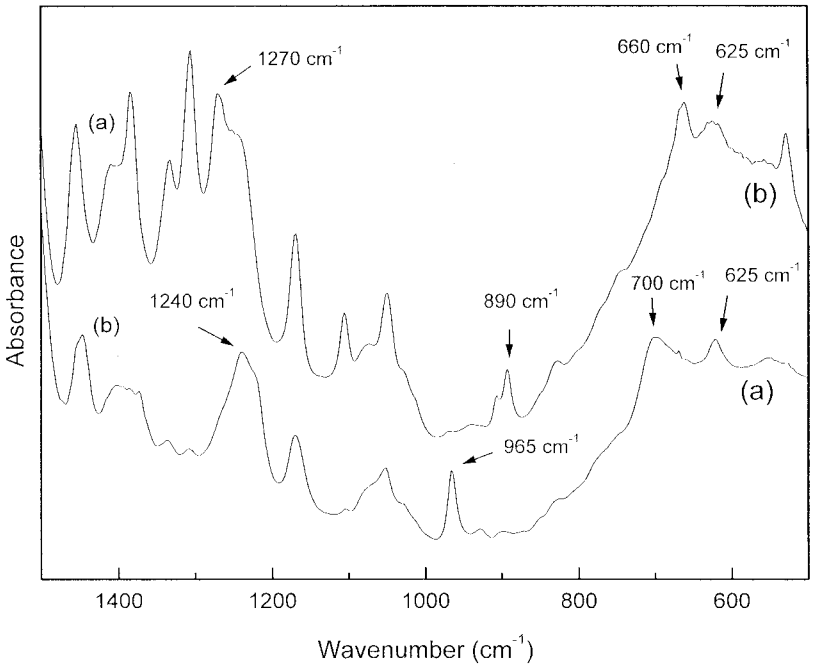

Figure 5 FTIR spectra of (a) *A. pernyi* silk fiber and (b) its regenerated film.

Solubility of silk fiber (wt %)

$$=(Wi - Wf)/Wi \times 100$$

where Wi is the initial weight of silk fiber (g), and Wf, the residue weight of the silk fiber on the nonwoven fabrics (g)

Preparation of Regenerated Film

The degummed silk fiber was dissolved in a 7*M* calcium nitrate solution at 100°C for 3 h. The dissolved solution was dialyzed in a cellulose tube (molecular cutoff = 3500) against distilled water for 4 days at room temperature and then cast onto

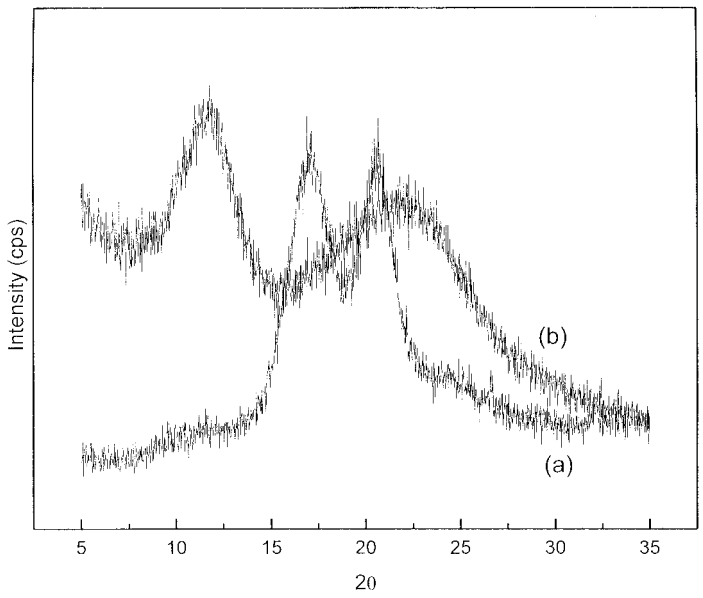

Figure 6 X-ray diffractograms of (a) *A. pernyi* silk fiber and (b) its regenerated film.

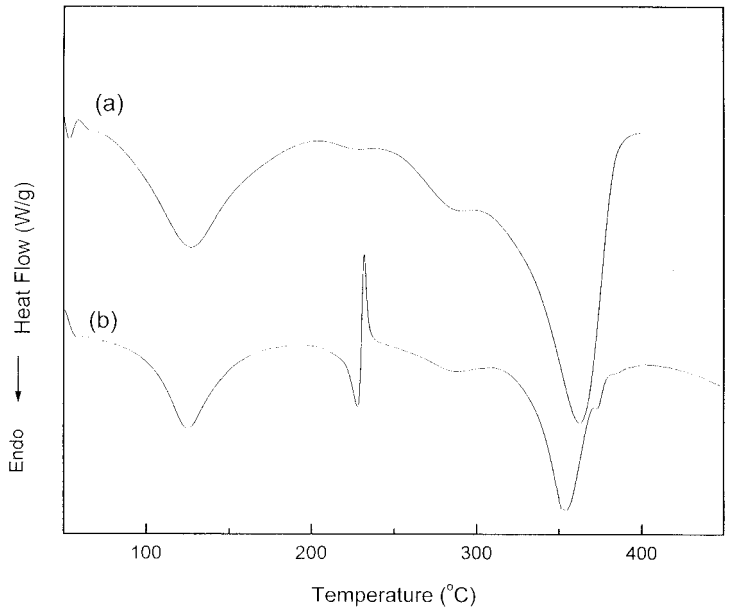

Figure 7 DSC thermograms of (a) *A. pernyi* silk fiber and (b) its regenerated film.

a polystyrene plate as the substrate at 20°C and 40% relative humidity. Film samples of around 30 μm were prepared.

Measurements

Polyacrylamide gel electrophoresis (PAGE) was performed according to Laemmli's method[6] on 12.5% polyacrylamide gels containing 0.1% sodium dodecyl sulfate (SDS) buffer. The proteins were stained with Coomasie Brilliant Blue R-250 (Sigma Chemical Co., St. Louis, MO).

FTIR spectra were obtained using a Midac M series spectrometer (USA) in the spectral region of 1400–500 cm^{-1}. The XRD curve was obtained using a D-MAX-3 diffractometer (Rigaku Co. Japan); CuKα radiation with a wavelength of 1.5418 Å was used. The scan speed was 0.5°/min and the range was 2θ = 5°–35° under 30 kV and 20 mA.

TGA was run under the flow of nitrogen gas at a scanning speed of 20°C/min using a Rheometric Scientific TGA 1000 (USA). DSC curves were obtained on a thermal analysis instrument (TA 2910, USA) at a heating rate of 10°C/min and a nitrogen gas flow rate of 50 mL/min.

Dynamic mechanical thermal properties were measured using a Rheometric Scientific DMTA Mark 4 (USA). The frequency of oscillation was adjusted to 1 Hz. The temperature range studied was from 100 to 250°C and the heating rate of the sample was 4°C/min.

RESULTS AND DISCUSSION

Solubility

Figure 1 represents the solubility of *A. pernyi* silk fiber dissolved in various concentrations of a calcium nitrate solution at 110°C for 3 h. *A. pernyi* silk fiber was nearly insoluble in a 5*M* calcium nitrate solution or less, soluble only in about a 20 wt % in a 6*M* solution, and nearly 100% soluble in a melt solution, at about 7*M* concentration. Even at a sufficiently high dissolving temperature of 110°C, at least 7*M* of calcium nitrate is required for complete dissolution.

A dissolving temperature can affect the dissolution of *A. pernyi* silk fiber. Figure 2 shows the solubility of *A. pernyi* silk fiber dissolved in a 7*M* calcium nitrate solution at various dissolving temperatures for 3 h. The value of the solubility was only about 10 wt % at 75°C. However, as the dissolution temperature increased to 100°C, the

Figure 8 TGA and DTG thermograms of silk fibroin: (a) regenerated *A. pernyi* silk fibroin film; (b) *A. pernyi* silk fiber; (c) *B. mori* silk fibroin.

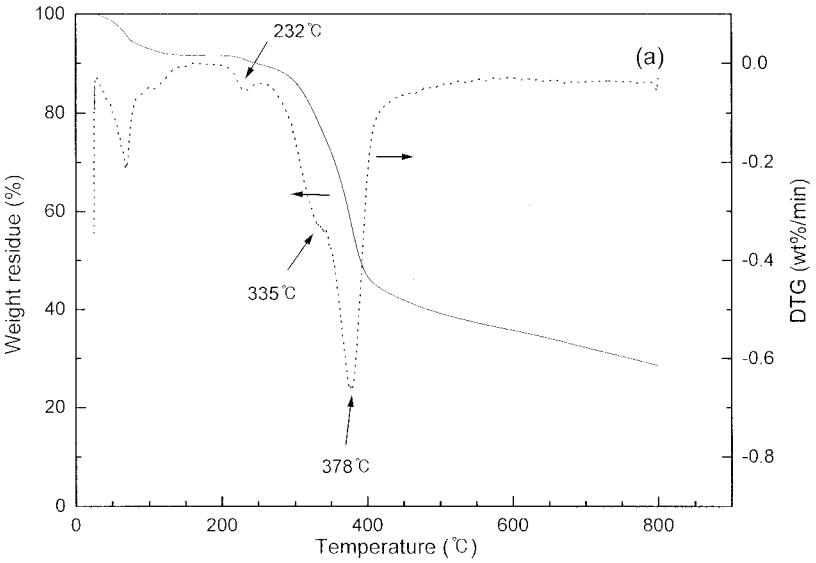
232℃
(a)
335℃
378℃
Weight residue (%)
DTG (wt%/min)
Temperature (℃)

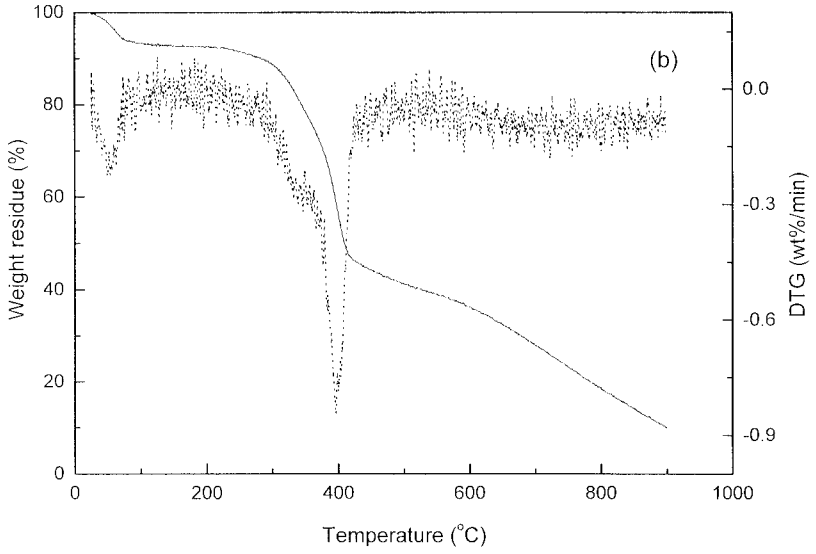
(b)
Weight residue (%)
DTG (wt%/min)
Temperature (°C)

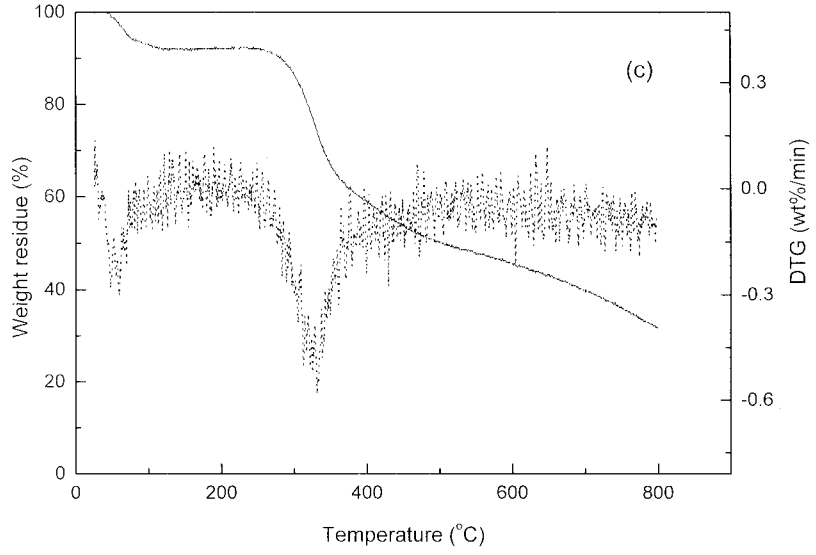
(c)
Weight residue (%)
DTG (wt%/min)
Temperature (°C)

solubility was increased linearly and about 90 wt % of the solubility could be obtained.

Figure 3 represents the dissolution rate of *A. pernyi* silk fiber in a 7*M* calcium nitrate solution. As expected, the dissolution rate curves were significantly affected by the dissolution time and temperature. Even when the dissolution time was prolonged to 12 h, the solubility of silk fiber at 80°C reached only about 55 wt %. According to this figure, it is recommended that the dissolving temperature should be at least 100°C for obtaining more than 90% solubility within 2 h.

As shown in Figures 1–3, the solubility was increased with a higher concentration of salt and dissolving temperature. However, the degradation of silk fibroin can occur when the dissolution conditions are severe. The color of the dissolving solution became dark brown, changing from pale yellow. The preferable dissolution conditions of *A. pernyi* silk fibroin are a 7*M* concentration of the calcium nitrate solution, 100°C temperature, and 3-h dissolving time.

Electrophoresis of Regenerated Solution

SDS–PAGE has been used to elucidate the molecular weight of protein by many researchers. Figure 4 shows the result of SDS gel electrophoresis of a regenerated *A. pernyi* silk fibroin aqueous solution. The electrophoresis pattern showed several stained regions above 14 kDa, suggesting that regenerated silk fibroin was composed of a mixture of polypeptides with several molecular weights.

The molecular weight of tussah silk fibroin, taken directly from the posterior division of the silk gland, is known to be 400–450 kDa, whose value decreased to 220 kDa by a reduction of the disulfide linkage.[7] Therefore, it can be concluded that *A. pernyi* silk fibroin was extensively depolymerized by scission of the main chains and resulted in the mixture composed of heterogeneous molecular weights. When the dissolution conditions are severe, regenerated film is not formed due to a low molecular weight induced by degradation.

FTIR Spectra

IR spectroscopy is a widely used technique to study the molecular conformation and crystalline structure of silk protein, because the position and intensity of the amide bonds are sensitive to the molecular conformation of fibroin. Figure 5 shows FTIR spectra of *A. pernyi* silk fiber and its regenerated film. *A. pernyi* silk fiber shows strong absorption bands at 1240 (amide III), 965, and 700 cm^{-1} (amide V), assigned to the β-sheet structure, and 625 cm^{-1} (amide V), α-helix conformation. On the other hand, regenerated silk fibroin film showed strong absorption bands at 1270 (amide III), 890, and 625 cm^{-1} (amide V), attributed to the α-helix conformation, and at 660 cm^{-1} (amide V), attributed to the random-coil conformation. The IR spectrum of the silk fiber and film is completely different due to the conformational change induced by dissolution.

For a dissolution process to work effectively, the solution of chaotropic salt first swells the amorphous part of the compact fibrous structure, breaks the inter/intrahydrogen bonds among the crystallines, and, finally, disperses into fibroin molecules. The conformational change induced by chaotropic salt from a crystalline to a random-coil structure was also reported in the case of *B. mori* silk fibroin.[8,9] Therefore, considering the IR spectra of regenerated silk fibroin film prepared from a chaotropic salt solution, the chaotropic salt solution may break the inter/intrahydrogen bonds among the crystalline structure and transform the conformation of silk fibroin from a β-sheet to a random-coil and an α-helix structure.

XRD Curves

XRD curves of *A. pernyi* silk fiber and its regenerated film are shown in Figure 6. Tussah silk fiber shows the typical characteristic peaks of β-sheet conformation for *A. pernyi* silk fibroin at about 16.4° and 20.0° corresponding to β-sheet crystalline spacing of 5.40, and 4.43 Å, respectively. On the other hand, the regenerated film is characterized by the presence of two peaks at 11.8° and 22.0°, corresponding to the α-helix crystalline spacing of 7.49 and 4.03 Å, respectively. These two peaks exhibit the same characteristics of native *A. pernyi* fibroin film, collected from the posterior division of the silk gland in full-grown larvae of the silkworm, with an α-helix crystalline structure.[10–12] The conformation of *A. pernyi* silk fibroin film regenerated from a lithium thiocyanate solution was also reported as an α-helix crystalline structure.[13]

The crystalline regions of *A. pernyi* silk fibroin are composed mainly of —$(ala)_n$— sequences. Poly(L-alanine), a model polypeptide for tussah silk fibroin, shows strong Debye–Scherrer rings corresponding to 7.40 and 3.69 Å, assigned to the

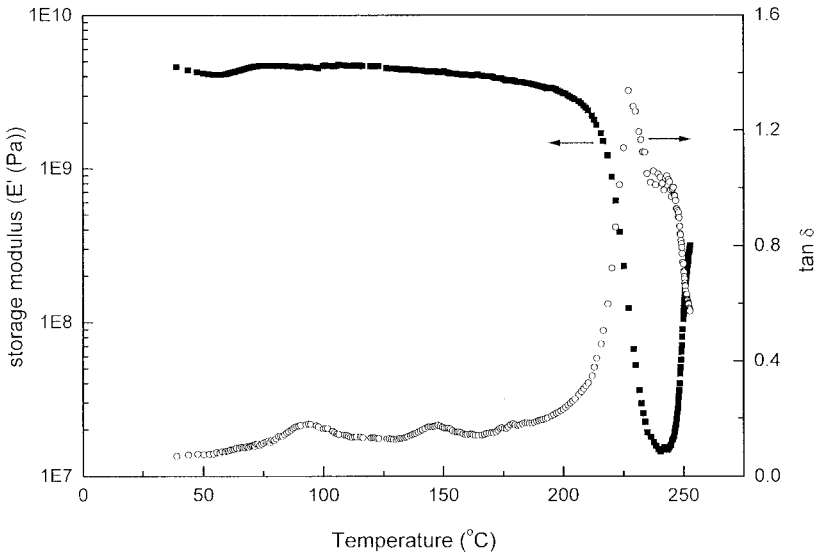

Figure 9 Dynamic storage modulus (E') and tan δ of regenerated *A. pernyi* silk fibroin film.

α-helix structure, and to 5.31, and 4.33 Å, assigned to the β-sheet structure.[14] The spacings of *A. pernyi* silk fiber and its regenerated film are somewhat larger in comparison with those of poly(L-alanine). This result can be interpreted to a certain degree of disorder existing within the crystalline region.

Thermal Properties

The thermal behavior of regenerated silk fibroin was investigated using DSC and TGA methods. Figure 7 shows the DSC curves of *A. pernyi* silk fiber and its regenerated film. The *A. pernyi* silk fiber showed two broad and large endothermic peaks about 100°C, due to the loss of moisture, and about 365°C, attributed to thermal degradation of a well-oriented β-sheet crystalline conformation.[15] On the other hand, regenerated film showed extra peaks of a sharp endotherm about 228°C and sharp exotherm about 232°C. It is known that the endotherm at 228°C is attributed to the strong molecular motion within the α-helix crystals, while the sharp exotherm at 232°C can be attributed to the crystallization during heating by forming the β-sheet structure from a random-coil conformation.[16] The broad and major endotherm at 355°C is due to the decomposition of fibroin molecules with unoriented β-sheet conformations.[13,15]

The DSC data are in good agreement with the IR spectra and XRD patterns, implying that regenerated silk fibroin film has a completely different structure from that of silk fiber owing to the reconformation of silk fibroin molecules induced by dissolution in a chaotropic salt solution. The thermogravimetric and differential thermogravimetric curves of regenerated fibroin films are shown in Figure 8(a). The weight loss below 150°C was known to be due to the evaporation of water. As the temperature increases, the weight loss (%) of regenerated film is proceeded step-by-step, depending on a certain temperature range. According to the TGA curves, thermal decomposition of regenerated *A. pernyi* fibroin film displays three main decomposition stages: the first step, a slight thermal decomposition of the silk fibroin molecules from 220 to 300°C; the second, an abrupt decomposition step from 300 to 370°C; and the third, from 370 to 400°C. The differential weight loss (DTG) curves provide clear evidence for the three degradation steps. The maximum degradation temperature of each step in regenerated fibroin film is obtained about 232, 355, and 378°C, respectively.

The weight loss and DTG curves of *A. pernyi* silk fiber, as shown in Figure 8(b), were not significantly changed from those of regenerated fibroin film. On the other hand, the thermal decomposition behavior of *B. mori* silk fibroin film is different from that of *A. pernyi* fibroin film. Figure 8(c) shows that the weight loss of *B. mori* fibroin film followed a simple single step of thermal decomposition.

Polymorphs of a crystalline structure and amino acid composition of *A. pernyi* silk fibroin

are different from those of *B. mori* silk fibroin. Therefore, the thermal degradation behavior is expected to be different between *B. mori* and *A. pernyi* silk fibroin. *A. pernyi* silk fibers and other silks belonging to the family of Saturniidae showed decomposition through several steps.[17,18] According to the conformation and crystalline structure obtained from the FTIR spectra (Fig. 5) and XRD curves (Fig. 6), the structure of regenerated film was much different from that of the *A. pernyi* silk fiber. In spite of the conformational difference between the regenerated film and the silk fiber, thermal decomposition and DTG curves of the regenerated film were not changed significantly from that of silk fiber, indicating that the change of conformation seems to be little affected by the thermal decomposition behavior.

DMTA

DMTA is known as a sensitive method to monitor side/main-chain motion in specific regions and local-mode relaxations of silk protein. The dynamic storage modulus (E') and mechanical damping (tan δ) of regenerated *A. pernyi* silk fibroin film are examined in Figure 9. The storage modulus begins to drop remarkably around 210°C, reaches a minimum about 240°C, and then finally increases. On the contrary, the loss tangent increases abruptly about 210°C, reaches a maximum about 227°C, and then decreases. After passing though a minor shoulder peak about 240°C, the loss tangent again decreases. The mechanical damping peak was somewhat lower than that of tussah silk fiber, around 260°C.[19]

In the glass transition region, some molecular chain segments were frozen-in while some were free to move. The damping peak is associated with partial loosening of the polymer structure so that groups and small-chain segments can move. The mechanical damping gives the amount of energy dissipated as heating during the deformation. In general, the mechanical damping peak is affected by the molecular orientation, crystallinity, and so on.[20]

REFERENCES

1. Sakabe, H.; Itoh, H.; Miyamoto, T.; Nishiki, Y.; Ha, W. S. Sen-i Gakkaishi 1989, 45, 487.
2. Minoura, N.; Tsukada, M.; Nagura, M. Polymer 1990, 31, 265.
3. Iizuka, E. J Appl Polym Sci Appl Poym Symp 1985, 41, 173.
4. Kweon, H. Y. Ph.D. Thesis, Seoul National University, 1998.
5. Matsumoto, K.; Uejima, H.; Iwasaki, T.; Sumino, H. J Appl Polym Sci 1996, 60, 503.
6. Laemmli, U. K. Nature 1970, 227, 680.
7. Tamura, T.; Kubota, T. In Wild Silkmoth; Arai, H., Ed.; National Institute of Sericulture and Entomological Science, Tsukuba, 1988; pp 67–72.
8. Goto, Y.; Tsukada, M.; Minoura, N. J Ser Sci Jpn 1990, 59, 402.
9. Bhat, N. V.; Ahirrao, S. M. J Polym Sci Polym Chem Ed 1983, 21, 1273.
10. Tsukada, M. J Polym Sci Polym Phys Ed 1986, 24, 1227.
11. Tsukada, M.; Freddi, G.; Monti, P.; Bertoluzza, A.; Kasai, N. J Polym Sci Polym Phys Ed 1995, 33, 1995.
12. Tsukada, M. J. Polym Sci Polym Phys Ed 1986, 24, 457.
13. Tsukada, M.; Freddi, G.; Gotoh, Y.; Kasai, N. J Polym Sci Polym Phys Ed 1994, 32, 1407.
14. Tsukada, M.; Nagura, M.; Ishikawa, H. J Polym Sci Polym Phys Ed 1987, 25, 1325.
15. Magoshi, J.; Magoshi, Y.; Nakamura, S.; Kasai, N.; Kakudo, H. J Polym Sci Polym Phys Ed 1977, 15, 1675.
16. Nagura, M.; Urushidani, M.; Shiohara, H.; Ishikawa, H. Kobunshi Ronbunshu 1978, 35, 81.
17. Kweon, H. Y.; Park, Y. H. Kor J Ser Sci 1994, 36, 138.
18. Kato, H. Int J Wild Silkmoth Silk 1994, 1, 84.
19. Nagura, M.; Yamazaki, S.; Tsukada, M. In Proceedings of the 7th International Wool Textile Research Conference, Tokyo, 1985; Vol. 1, p 345.
20. Murayama, T. Dyanmic Mechanical Analysis of Polymer Material; Elsevier: New York, 1978; Chapter 3.